Biogeosciences Discuss., 12, 7705–7737, 2015
www.biogeosciences-discuss.net/12/7705/2015/
doi:10.5194/bgd-12-7705-2015

Biogeosciences Discussions
Open Access

Iron encrustations on filamentous algae colonized by *Gallionella*-related bacteria in a metal-polluted freshwater stream

J. F. Mori[1], T. R. Neu[2], S. Lu[1,3], M. Händel[4], K. U. Totsche[4], and K. Küsel[1,3]

[1]Institute of Ecology, Aquatic Geomicrobiology, Friedrich Schiller University Jena, Dornburger Strasse 159, 07743 Jena, Germany
[2]Department of River Ecology, Helmholtz Centre for Environmental Research – UFZ, Brueckstrasse 3A, 39114 Magdeburg, Germany
[3]German Centre for Integrative Biodiversity Research (iDiv) Halle-Jena-Leipzig, Deutscher Platz 5e, 04103 Leipzig, Germany
[4]Institute of Geosciences, Hydrogeology, Friedrich Schiller University Jena, Burgweg 11, 07749 Jena, Germany

Received: 17 April 2015 – Accepted: 2 May 2015 – Published: 22 May 2015

Correspondence to: K. Küsel (kirsten.kuesel@uni-jena.de)

Published by Copernicus Publications on behalf of the European Geosciences Union.

Abstract

Filamentous macroscopic algae were observed in slightly acidic to circumneutral (pH 5.9 ~ 6.5) metal-rich stream water that leaked out in a former uranium-mining district (Ronneburg, Germany). These algae differ in color and morphology and were encrusted with Fe-deposits. To elucidate the potential interaction with Fe(II)-oxidizing bacteria (FeOB), we collected algal samples at three time points during summer 2013 and studied the algae-bacteria-mineral compositions via confocal laser scanning microscopy (CLSM), scanning electronic microscopy, Fourier transform infrared spectra, and a 16S and 18S rRNA gene based bacterial and algae community analysis. Surprisingly, sequencing analysis of 18S rRNA gene regions of green and brown algae revealed high homologies with the yellow-green freshwater algae *Tribonema* (99.9 ~ 100 %). CLSM imaging indicates a loss of active chloroplasts in the algae cells, which may be responsible for the change in color in *Tribonema*. Fe(III)-precipitates on algal cells identified as ferrihydrite and schwertmannite were associated with microbes and extracellular polymeric substances (EPS)-like glycoconjugates. While the green algae were fully encrusted with Fe-precipitates, the brown algae often exhibited discontinuous series of precipitates. This pattern was likely due to the intercalary growth of algal filaments which allowed them to avoid fatal encrustation. 16S rRNA gene targeted studies based on DNA and RNA revealed that *Gallionella*-related FeOB dominated the bacterial RNA and DNA communities (70–97 and 63–96 %, respectively) suggesting their contribution to Fe(II) oxidation. Quantitative PCR revealed higher *Gallionella*-related 16S rRNA gene copy numbers on the surface of green algae compared to the brown algae. The latter harbored a higher microbial diversity, including some putative predators of algae. Lower photosynthetic activities of the brown algae lead to reduced EPS production which may have enabled predator colonization. The differences observed between green and brown algae suggest that metal-tolerant *Tribonema* sp. provide suitable microenvironments for microaerophilic Fe-oxidizing bacteria. However, high levels of iron orchres can be fatal to the alga.

BGD
12, 7705–7737, 2015

1 Introduction

Algae are known to inhabit all freshwater ecosystems including rivers, streams, lakes and even small water volumes present in pitcher plants (Stevenson et al., 1996; Cantonati and Lowe, 2014; Gebühr et al., 2006). Macroscopic algae often bloom rapidly in rivers and in small freshwater streams, such as groundwater effluents (Stevenson et al., 1996), through germination of spores, vegetative growth and reproduction (Transeau, 1916). As primary producers these algae provide benefits for other organisms by supplying them with organic matter and oxygen via photosynthesis and are often surrounded by associated microbes (Haack and McFeters, 1982; Geesey et al., 1978; Cole, 1982; Azam, 1998). Unicellular and multicellular algae can produce polysaccharides like extracellular polymeric substances (EPS) as a shunt for carbon produced in excess during photosynthesis, especially during cell senescence (Wotton, 2004; Liu and Buskey, 2000). Due to these functions, algae likely affect the activities of co-existing microbes and play important roles in microbial ecology in streams.

Some algal species have been detected in metal-polluted streams, such as hot spring effluents (Wiegert and Mitchell, 1973) and mining-impacted sites (Reed and Gadd, 1989; Warner, 1971). These algae are known to be tolerant or resistant to high concentration of metals such as Zn, Cu, Cd, Pb, Fe, and As (Reed and Gadd, 1989; Foster, 1977, 1982) and some are capable of accumulating metals (Fisher et al., 1998; Yu et al., 1999; Greene et al., 1987) which makes them ideal candidates for bioremediation of metal-polluted sites (Yu et al., 1999; Malik, 2004). Green algae, such as *Ulothrix*, *Microspora*, *Klebsormidium*, and *Tribonema,* occur in acid mine drainage (AMD)-impacted sites (Warner, 1971; Winterbourn et al., 2000; Das et al., 2009), sometimes forming heterogeneous streamer communities (Rowe et al., 2007). Although some of these algae show iron ochre depositions, their interactions with Fe(II)-oxidizing bacteria are not well characterized.

A group of prokaryotes called Fe(II)-oxidizing bacteria (FeOB) mediates the oxidation of Fe(II) to Fe(III) to conserve energy for growth (Colmer and Hinkle, 1947; Hanert,

BGD
12, 7705–7737, 2015

1981). Most FeOB are autotrophs (Johnson and Hallberg, 2009; Kappler and Straub, 2005). Biogenic Fe(III) subsequently hydrolyzes and precipitates from solution forming various Fe(III)-oxides when the pH exceeds 2 (C. A. Johnson et al., 2014). Aerobic acidophilic Fe(II)-oxidizers are the main drivers for Fe(II)-oxidation in acidic and iron-rich freshwater environments due to low rates of chemical Fe(II)-oxidation under acidic conditions (Leduc and Ferroni, 1994; Hallberg et al., 2006; Tyson et al., 2004; López-Archilla et al., 2001; Senko et al., 2008; Kozubal et al., 2012). In contrast, neutrophilic FeOB, such as *Gallionella* spp., *Sideroxydans* spp., or *Leptothrix* spp., have to compete with a rapid chemical Fe(II)-oxidation at circumneutral pH and thus often inhabit oxic-anoxic transition zones, such as sediment-water surfaces (Emerson and Moyer, 1997; Peine et al., 2000; Hedrich et al., 2011b), or the rhizosphere of wetland plants, where the plant roots leak oxygen and FeOB deposit Fe-minerals (known as "Fe-plaques") on plant root surfaces (Neubauer et al., 2002; Johnsongreen and Crowder, 1991; Emerson et al., 1999). *Gallionella* spp. are chemolithoautotrophs that prefer microoxic conditions with 13–20 % oxygen saturation (Emerson and Weiss, 2004; Lüdecke et al., 2010).

Acidophilic and neutrophilic FeOB can produce EPS, which can be used to protect the cells against encrustation with Fe(III)-minerals by acting as a barrier to prevent accumulation of Fe(III)-minerals directly on cell surfaces. This defense mechanism is especially important for FeOB growing above pH 2. EPS can also accelerate bacterial Fe(II)-oxidation by catching free Fe(II) in the water and localizing microbially formed Fe-oxides in proximity to the cells, which allow bacteria to utilize the proton gradient for energy generation (Chan et al., 2004). EPS-producing acidophilic FeOB, such as *Acidithiobacilllus* spp., *Ferrovum* spp., *Leptospirillum* spp., and *Acidimicrobium* spp., are known for their gelatinous, filamentous macroscopic growth in flowing waters (Wakao et al., 1985; Bond et al., 2000; Hallberg et al., 2006; Kay et al., 2013). Recently, a pure culture of *Ferrovum myxofaciens* was shown to produce copious amounts of EPS, composed mainly of polysaccharides and proteins, which allows the cells to attach to each other and solid surfaces, preventing the cells from being washed out in

BGD
12, 7705–7737, 2015

flowing systems (D. B. Johnson et al., 2014). This streamer-like growth appears to be particularly important in extreme environments.

We observed macroscopic streamer-forming algae in slightly acidic to circumneutral (pH 5.9 ~ 6.5), metal-rich stream water flowing out of passively flooded abandoned underground mine shafts in the former Ronneburg uranium mining district in Germany. This seeping groundwater creates new streams and iron-rich terraces at an adjacent drainage creek bank. The filamentous algae present during the summer months differed mainly in color, but all types showed iron ochre deposits. Since high abundances of *Gallionella*-related FeOB were detected in the seeping water and the drainage creek in a previous studies (Fabisch et al., 2013, 2015), potential interactions between these neutrophilic FeOB and the streamer-forming algae communities were suggested. Thus, we applied different microscopic techniques to localize the Fe-minerals and microorganisms on the algal surfaces and compared the bacterial community structure of different algal samples to learn more about these multi-species interactions in metal-polluted environments.

2 Materials and methods

2.1 Field site and sampling

Algal samples were taken in the outflow water in the former Ronneburg uranium-mining district (Thuringia, Germany) in 2013. This district in eastern Germany was one of the largest uranium mining operations in the world which produced 113 000 metric tons of uranium primarily through heap-leaching with sulfuric acid between 1945 and German reunification in 1990. After the mines were closed, the open pit was filled with waste rock from the leaching heaps to prevent further acid mine drainage (AMD). The underground mines were flooded and treated with alkali to buffer the water to a more neutral pH. The mine water outflow began in 2010 when the water table rose and contaminated water from the underground mine reached the surface of surrounding

BGD
12, 7705–7737, 2015

grassland. The mine water outflow flowed 20 m down a hillside into the creek (Fig. 1) where red-orange terraces enriched with Fe-oxyhydroxides goethite and ferrihydrite formed (C. A. Johnson et al., 2014; Fabisch et al., 2015).

We sampled algae of green and brown color in July, August and September from four different sites beginning at the outflow water (site O) and three sites further downstream (A, B, C) which were separated from O by some artificial impoundments; the distance between A and C was 8.8 m (Fig. 1). Chemical parameters of water (pH, temperature, Eh, and oxygen concentration) were measured in situ at every sampling time, using respective electrodes and meters (Mettler Toledo; WTW, Switzerland). In addition, water collected from each site was filtered with 0.45 µm PVDF and acidified with HCl or HNO_3 on site and stored at 4 °C until the measurements of metals, sulfate, and organic carbon (DOC) concentrations. Algae and sediment samples were taken from the stream with a sterilized spatula and stored at 4 °C for microscopic analyses or at −80 °C for molecular biological experiments, respectively.

2.2 Geochemical characterization of the stream

Concentration of Fe(II) in water was detected with the phenanthroline method (Tamura et al., 1974) and total Fe was determined after the addition of ascorbic acid (0.6 % final concentration). Sulfate concentration was determined using the barium chloride method (Tabatabai, 1974). DOC in water was measured by catalytic combustion oxidation using TOC analyzer (TOC-V CPN, Shimadzu, Japan). Dissolved metals (Fe, Mn, Ni, and U) in stream water were measured using inductively coupled mass spectrometry (ICP-MS; X-Series II, Quadrupol, Thermo Electron, Germany). Metals which accumulated on the sediments and the algae were determined by ICP-MS and ICP-optical emission spectrometry (ICP-OES, 725ES, Varian, Germany) after digestion. The algae sample taken at site C in August 2013 and stored at 4 °C was washed with deionized water on a petri dish to remove big sediment particles, then followed by drying (200 °C, overnight), grinding and microwave digestion (Mars XPress, CEM, Germany) using HNO_3 for ICP-MS/OES measurements. The sediment samples taken at

BGD
12, 7705–7737, 2015

each sampling site were also dried and ground, and then 0.1–0.5 g of sediments were digested using 2 mL HNO_3, 3 mL HF, and 3 mL $HClO_4$ for ICP-MS/OES measurements.

2.3 Observation of algae under light microscope

The fresh algal samples were observed just after sampling under light microscope (Axioplan, Zeiss, Germany). Small pieces (~ 5 mm) of algal bundles were picked, placed on a glass slide with small amount of stream water, and then covered with a glass coverslip. Microscopic images were taken with digital camera ProgRes CS (Jenoptik, Germany).

2.4 CLSM imaging

The algal samples taken in September were examined by confocal laser scanning microscopy (CLSM) using a TCS SP5X (Leica, Germany). The upright microscope was equipped with a white laser source and controlled by the software LAS AF version 2.4.1. Samples were mounted in a 0.5 µm deep CoverWell™ (Lifetechnologies) chamber and examined with a 63 × NA 1.2 water immersion lens. Algal-associated bacteria were stained nucleic acid specific fluorochrome Syto9. Fluorescently labelled lectin (AAL-Alexa448, Linaris), which can be applied for detection of algal cell walls (Sengbusch and Müller, 1983) and the microbial EPS complex (Neu et al., 2001), was used to stain and detect glycoconjugates. The recording parameters were as follows: excitation at laser lines 488, 568, 633 nm; emission recorded at 483–493 (reflection), 500–550 (Syto9), 580–620 (possible autofluorescence), 650–720 (chlorophyll *a*). Optical sections were collected in the *z* direction with a step of 1 µm. Images were deconvolved using the option "classic maximum likelihood estimation" from Huygens version 14.06 (SVI). Lastly, image data sets were projected by Imaris version 7.7.2 (Bitplane).

BGD
12, 7705–7737, 2015

2.5 SEM-EDX

Scanning electron microscopy (SEM) was used to study the morphology of mineral precipitates on algal surfaces. Droplets of sample suspensions were placed on silicon wafers and subjected to air drying. High-resolution secondary electron (SE) images and energy dispersive X-ray spectroscopy (EDX) were taken with an ULTRA plus field emission scanning electron microscope (Zeiss).

2.6 FTIR measurement for mineral precipitates on algae

Fourier transform infrared (FTIR) spectra of algae encrusted with Fe-minerals were recorded using a Nicolet iS10 spectrometer (Thermo Fisher Scientific, Dreieich, Germany). Mortared samples were mixed with KBr (FTIR grade, Merck, Darmstadt, Germany) at a ratio of 1 : 100 and pressed into pellets. The pellets were studied in transmission mode in the mid-infrared range between 4000 and 400 cm^{-1} for a total of 16 scans at a resolution of 4 cm^{-1}. Spectra were baseline corrected by subtracting a straight line running between the two minima of each spectrum and normalized by dividing each point by the spectrum's maximum.

2.7 Total nucleic acids extraction from algae-microbial communities

Total nucleic acids of algae-microbial communities were extracted from ~ 1.4 g wet weight of algal bundle via bead beating in $NaPO_4$ buffer (pH 8.0) with TNS solution (500 mM Tris-HCl pH 8.0, 100 mM NaCl, 10 % SDS wt/vol). The supernatant was taken after centrifugation, followed by extraction with equal volumes of phenol-chloroform-isoamyl alcohol [PCI, 25 : 24 : 1 (vol : vol : vol), AppliChem] and chloroform-isoamyl alcohol [CI, 24 : 1 (vol : vol), AppliChem]. Nucleic acids were precipitated with two volumes of polyethylene glycol (PEG) by centrifugation at 20 000 *g* and 4 °C for 90 min. The pellets were washed with ice-cold 70 % ethanol and suspended in 50 µL elution buffer (EB, Qiagen).

BGD
12, 7705–7737, 2015

2.8 18S rRNA gene-based identification of algal species

The 18S rRNA gene region of the DNA extracted from algae-microbial communities was amplified by PCR employing the universal primer pair Euk20F/Euk1179R (Euringer and Lueders, 2008) or the *Chlorophyta*-targeting primer pair P45/P47 (Dorigo et al., 2002). The PCR reactions using both primer pairs were as follows: initial denaturing at 94 °C for 5 min, 25–30 cycles of denaturing at 94 °C for 30 s, annealing at 57 °C for 30 s, and extension at 72 °C for 90 s, and followed by final extension at 72 °C for 10 min. Amplified products were purified through a spin column (NucleoSpin Gel and PCR Clean-up, Macherey-Nagel, Germany) and sequenced (Macrogen Europe, Amsterdam, the Netherlands). Sequences were processed using Geneious 4.6.1 for trimming and assembling, followed by the BLAST homology search.

2.9 Quantitative PCR

Quantitative PCR was performed to elucidate the 16S rRNA gene copy numbers of *Gallionella* colonizing the algae surface using 16S rRNA gene-targeted primers specific for *Gallionella* spp. (Gal122F, 5'-ATA TCG GAA CAT ATC CGG AAG T -3'; Gal384R, 5'- GGT ATG GCT GGA TCA GGC -3') (Heinzel et al., 2009). Aliquots of 1.25 ng DNA were used in triplicate as the template for qPCR using the Mx3000P real-time PCR system (Agilent, USA) and Maxima SYBR Green qPCR Mastermix (Fermentas, Canada). Standard curves were prepared by serial dilution of plasmid DNA containing the cloned 16S rRNA gene sequence of *Gallionella* (accession no. JX855939). Melting curve analysis was used to confirm the specificities of the qPCR products. PCR grade water and TE buffer were included as non-template controls. Detailed qPCR conditions were described by Fabisch et al. (Fabisch et al., 2013).

BGD
12, 7705–7737, 2015

2.10 Amplicon pyrosequencing

16S rRNA gene-targeted amplicon pyrosequencing was performed to reveal the population structures of bacteria on the algae. To determine the bacterial community composition based on RNA, cDNA samples were prepared as follows: 3.3–6.0 µg of total nucleic acids extracted from algae-microbial communities were treated with DNase using TURBO DNA-*free*™ Kit (Ambion, USA) to remove all DNA, and then 0.3–0.5 µg of DNase-treated RNA samples were transcribed to cDNA using RETROscript® Kit (Life Technologies, CA) and stored at −20 °C. The total nucleic acid samples (as DNA samples) and cDNA samples were sent to the Research and Testing Laboratory (Lubbock, TX, USA) for pyrosequencing of the V4-V6 region. Samples were sequenced on a Roche 454 FLX system using tags, barcodes and forward primers listed in Table S1. Sequence reads were processed in Mothur 1.33.0 (Schloss et al., 2009) for trimming, quality checking, screening, chimera removal, and alignment based on the Silva reference alignment files provided on the Mothur website (http://www.mothur.org/wiki/Silva_reference_files). Dendrograms were constructed in Mothur using unweighted pair group method arithmetic averages (UPGMA) based on Bray–Curtis index (Bray and Curtis, 1957) to estimate similarity among bacterial DNA and RNA community compositions in each sample. Sequences originating from algal chloroplasts were removed for statistical analysis of community composition. Gini–Simpson index was calculated using Mothur.

3 Results

3.1 Characterization of algae-bacterial assemblage

Abundant macroscopic filamentous algae up to 10 cm length appeared at the outflow site (O) (Fig. 1) and further downstream at sites A, B, and C during the summer months. Algae were often covered by orange-colored minerals. The outflow water was suboxic

BGD
12, 7705–7737, 2015

(1.3–2.0 mg L^{-1} oxygen) at site O with a slightly acidic pH of 5.9, however, water became more oxygenated (6.2–6.9 mg L^{-1} oxygen) and had a higher pH (6.4–6.5) further downstream (Fig. 2). Increase in oxygen and pH could be caused by photosynthetic activities of the algae and degassing of CO_2 from the initial anoxic outflow water. Water temperature was approximately 14–17 °C at site O during sampling; these water temperature values are likely due to the underground exothermic pyrite oxidation (C. A. Johnson et al., 2014). Dissolved iron in the water was primarily in the form of Fe(II) with maximum concentrations of 3.3 mM and decreased in concentration (to 2.1 mM) as the water moved downstream towards sites A, B, and C. The other parameters measured did not indicate distinct differences between the sites O, A, B, and C (Eh, 140–180 mV; conductivity, 4.8–4.9 ms cm^{-1}; DOC, 3.0–4.5 mg L^{-1}; sulfate concentration, 30–35 mM; Fig. 2). The stream water was also enriched with other metals including Mn, Ni, Zn and U.

In July 2013, we sampled green algae from sites A and B (algae at site O could not be reached), and brown algae from site C. During a subsequent sampling during August 2013, the algae collected from site B changed in color from green to brown, while algae samples collected from sites O and A still appeared green. By September 2013, most algae had disappeared; only small amounts of green algae were left at site O and some brown algae at site A (Table 1). Sequencing analysis of 18S rRNA gene regions amplified from DNA extracts of green and brown algae showed that all algae had high homologies with *Tribonema* sp. (*T. viride*, *T. minus*, *T. ulotrichoides*, 99.9 ~ 100 %; Table S2), a species of yellow-green freshwater algae belonging to the class of *Xanthophyceae*.

Microscopic observations revealed unbranched filamentous algae with a single cell length of 30–50 µm and a cell diameter of 8–10 µm (Figs. 3c, d and 4a–c). Green algae cells yielded 10–15 visible chloroplasts which exhibited strong auto fluorescence, whereas brown algae cells contained only 5–7 countable chloroplasts and displayed weaker auto fluorescence. The brown algae often showed green autofluorescence under UV-light exposure (data not shown), which likely resulted from flavin-like molecules

BGD
12, 7705–7737, 2015

or luciferin compounds (Tang and Dobbs, 2007). This green autoflouresence was not detected in the green algae, likely due to stronger signals from chloroplasts. According to the cell morphology and number of chloroplasts per cell, the green and brown algae display a high degree of similarity to *T. viride* (Akiyama et al., 1977; Gudleifsson, 1984; Wang et al., 2014).

Minerals adhered to and were distributed in a regular discontinuous pattern on the surface of the brown algae, however, the surface of the green algae was encrusted in a random arrangement and with roughly shaped minerals (Figs. 3c, d, and 4a, b). CLSM images using Syto9 stain showed minerals adhered to the surface of both brown and green algae were colonized by microorganisms (Fig. 4a and b). These microbial cells primarily colonized the minerals attached to the algae surfaces, while a smaller proportion of microbial cells were adhered directly to the algae bodies (or thin layer of minerals on the algae). CLSM images with lectin staining showed the cell sections in algal filaments were distributed between regularly located Fe-minerals. In addition, algal or bacterial EPS-like glycoconjugates which were likely associated with the minerals (Fig. 4c).

3.2 Component analysis of mineral precipitates on the algae

Secondary electron (SE) images with EDX analyses showed S-containing Fe-oxides almost completely covered the surface of the green algae (Figs. 5a and 6a), whereas some parts of the brown algae were not encrusted (Figs. 5b and 6b). The non-encrusted parts of the brown algae primarily displayed background signal (i.e. Si signal of the sample holder). Weak signals of C, Mg, Ca and P were also detected by EDX. The elemental composition of Fe-oxides not associated with algae was almost identical to those of the encrusted algae, suggesting mineral composition was not affected by biological activity.

FTIR spectra exhibited signals of ferrihydrite and schwertmannite (Fig. 6c). Their presence was also confirmed by high resolution SE images. Spherical aggregates with nano-needles on the surface edges are defining characteristics for schwertmannite

BGD
12, 7705–7737, 2015

(Fig. S1), while aggregates with no single crystallites are often composed of ferrihydrite (Carlson et al., 2002). The FTIR spectra of minerals on the green algae also showed weak signals of Si-O bonding at 1030 cm^{-1}, which might be due to residual clay minerals.

Total extractions of the brown algae collected at site C revealed that in addition to Fe, Mn, Ni, Zn and U accumulated on the algae surface similarly to the underlying sediments at site C (Fig. S2); Fe and U even showed higher concentrations on the surface of the algae in comparison to the sediment (540 mg of Fe and 910 µg of U in 1 gdw algae and 390–660 mg of Fe and 90–750 µg of U in 1 gdw sediment).

3.3 Elucidating the bacterial community structure associated with algae

Quantitative PCR detected high gene copy numbers (per gram wet weight algae) for *Gallionella*-related 16S rRNA with slightly higher numbers for the green algae (1.72×10^9–7.08×10^9) compared to brown algae (Table 1). Similarly, 16S rRNA gene-targeted amplicon pyrosequencing revealed that members of the *Gallionellaceae* were the dominant bacterial group within these algae-microbial communities when comparing both DNA and RNA samples from the green and brown algae collected at all four different sites and all time points (Fig. 7, Table S3). The relative percentage of *Gallionellaceae* was highest in RNA and DNA extracts of the green algae with 89.4–96.5 % and 79.5–96.4 %, respectively, of the total number of sequence reads compared to 70.4–82.9 % and 62.7–81.0 % in RNA and DNA extracts of the brown algae. Algal samples collected from sites O, A, B, and C during September showed the lowest fraction of *Gallionellaceae*. The *Gallionellaceae* group comprised of 2 OTUs related to the FeOB *Gallionella capsiferriformans* ES-2 (CP002159) and *Sideroxydans lithotrophicus* ES-1 (CP001965) (Table S3). The relative fraction of OTU-1-related FeOB was highest at site O, whereas OTU-2-related FeOB was more abundant downstream at sites A, B, and C. The dendrograms for each DNA and RNA community also showed that the bacterial community structures in site O were separated from those in other sites (Fig. 7). Other bacterial groups detected with less than 10 % relative abundance were "*Candi-*

BGD
12, 7705–7737, 2015

datus Odyssella" (Alphaproteobacteria), *Actinomycetales* (Actinobacteria), *Desulfobulbaceae*, and *Geobacteraceae* (Deltaproteobacteria). Triplicate extractions of DNA and RNA from the brown algae collected at site C in August showed little variation between bacterial community structures (Fig. 7), which allows for the identification of a representative algae surface-associated microbial community in this metal-contaminated site. The brown algae were colonized by a higher diversity of bacterial groups than the green algae, showing higher average Gini–Simpson index values (0.862 in RNA and 0.884 in DNA) than those of the green algae (0.641 in RNA and 0.645 in DNA). Interestingly, some of the sequences detected from the microorganisms adhered to the brown algae surface were identified as putative predators of algae, such as "*Candidatus* Odyssella" (intracellular parasite of Acanthamoeba, up to 8.1 and 6.0 % of OTUs in RNA and DNA extracts) and *Cystobacteraceae* (Myxobacteria, 2.0 and 0.2 % in RNA and DNA extracts).

4 Discussions

Members of the genus *Tribonema* are known as common freshwater algae (Machova et al., 2008; Wang et al., 2014). *Tribonema* species have been detected in other metal-rich and acidic freshwater environments such as acidic brown water streams (pH < 4) in New Zealand (Collier and Winterbourn, 1990), acidic coal mine drainage-contaminated sites (pH 2.6–6.0) (Winterbourn et al., 2000), as well as acidic rivers (pH 2.7–4.0) with iron-rich ochreous deposits of schwertmannite-like Fe-minerals on algal surfaces (Courtin-Nomade et al., 2005), suggesting their tolerance to high concentrations of metals and low pH. In this study, *T. viride* colonized metal-rich (Fe, Mn, Ni, Zn and U) and less acidic mine-water outflow with pH 5.9 to 6.5. The algae ostensibly changed its color from green to brown and disappeared completely from sites B and C at the end of the summer. The change in algae color occurred simultaneously with the loss of active chloroplasts per cell, as observed via CLSM imaging. These results correspond with lower numbers of sequences originating from chloroplasts based on sequences

BGD
12, 7705–7737, 2015

analysis. The encrustation with Fe-minerals presumably inhibits algal photosynthetic activities and may be an underlying cause for the disappearance of *Tribonema* at the end of the summer when light intensity diminished. The observed water temperatures (14–17 °C) may have also contributed to the decline in algae numbers, since optimal growth temperatures of two genera of *Tribonema* are higher (*T. fonticolum*, 19–27 °C; *T. monochloron*, 15.5–23.5 °C) (Machova et al., 2008), however, *T. viride* has been detected lake water with low temperature (0–5.6 °C) (Vinocur and Izaguirre, 1994).

Deposition of Fe-minerals and colonization of "iron bacteria" on *Tribonema* was reported more than 70 years ago (Chapman, 1941), but identification of the deposited minerals, the FeOB, and their interaction with the alga has not been characterized in detail. A symbiotic relationship has been suggested in which microbes living on the surface of *Tribonema* obtain their oxygen for Fe(II)-oxidation from algal photosynthesis and form ferric carbonate, which in turn controls water pH and acts as local buffer for the algae. We could not detect ferric carbonates on *Tribonema,* however, poorly crystalline iron minerals ferrihydrite and schwertmannite that are also present in the underlying sediments in addition to goethite were detected (C. A. Johnson et al., 2014). These iron minerals have a high reactive surface area for metal(loid) uptake, and particularly As and Zn appear to be associated with these minerals in the sediments (C. A. Johnson et al., 2014). Brown algae showed similar metal(loid) uptake to the sediments collected at the outflow downstream to site C with even higher concentrations for Fe and U suggesting a high affinity of *Tribonema* for these compounds.

Our microscopic investigation did not reveal a preferential colonization of microbes on the algal surface but on the minerals. According to both pyrosequencing and qPCR results, microaerophilic *Gallionella*-related FeOB were the dominant colonizers on *Tribonema* which might be due to the presence of large populations of *Gallionella* sp. (29–58 % of the total bacterial community) in the outflow water reaching cell numbers of 10^5 to 10^6 cells per mL water (Fabisch et al., 2015). These bacteria seem to be able to cope with the high levels of oxygen produced during photosynthesis, but these oxygen concentrations may be lower within the EPS matrix and ochre de-

BGD
12, 7705–7737, 2015

posits. *G. capsiferriformans*-related FeOB predominated at the outflow site whereas *S. lithotrophicus*-related FeOB dominated algae further downstream which can be explained by differences in the water geochemistry. 16S rRNA gene copy numbers of *Gallionella* on the algae surfaces (Table 1) were much higher than numbers found in the sediments of the stream (3.1×10^8 copies per gram wet weight sediment) (Fabisch et al., 2015).

The high relative RNA-derived fraction of *Gallionellaceae* suggested not only passive or active colonization of the algal surface but also participation in Fe-oxidation followed by ferrihydrite and schwertmannite formation. *Gallionella*-related FeOB appeared to be more abundant and active on the green algae, which indicates higher Fe-oxidizing activity on the surface of green algae. Most bacteria associated with the Fe-minerals were also localized the areas where EPS-like glycoconjugates were detected. The EPS forms a suitable microenvironment for microbial Fe-oxidation due to its ability to bind dissolved Fe(II) resulting from the negatively charged EPS matrix. This activity leads to the inhibition of chemical Fe-oxidation by lowering the availability of Fe(II) (Neubauer et al., 2002; Jiao et al., 2010; Roth et al., 2000). In addition, the EPS can prevent bacterial cells from being encrusted with insoluble Fe(III)-oxides (Neubauer et al., 2002; Hedrich et al., 2011a). Unfortunately, with the methods used, we could not determine if the EPS-like matrix on the algae was produced by the alga or by bacteria. *Tribonema* is known to produce EPS mainly composed of glucans and xylans (Cleare and Percival, 1972), however, based on genome sequencing both *G. capsiferriformas* ES-2 and *S. lithotrophicus* ES-1 are predicted to produce EPS (Emerson et al., 2013). In an effort to prevent encrustation, other *Gallionella* species form long stalks composed of polysaccharides where Fe-oxides are deposited (Fabisch et al., 2015; Hanert, 1981). Stalk-forming *Gallionella* have been isolated in sediment environments, but not on the surface of algae which implies EPS plays an important role for microbial Fe-oxidation by the algae-associated bacteria. The variations in color of the *Tribonema* species were accompanied with a variation in encrustation patterns. The green *Tribonema* was fully encrusted whereas the brown *Tribonema* showed an irregular encrustation pattern. Al-

BGD
12, 7705–7737, 2015

though *Tribonema* appears to be adapted to high metal loads, excess encrustations with Fe-minerals should be fatal due to inhibition of photosynthesis and decreased access to nutrients. The lower number of chloroplast pointed to decreased photosynthetic activity of the brown *Tribonema*. The discontinuous encrustation might be caused by intercalary growth of the filamentous algae, which occurs by generating H-shaped parts in the middle of each cell (Smith, 1938). Intercalary growth was confirmed by CLSM images with lectin staining which showed algal cell sections alternating with Fe-minerals. The new cell sections were thin with only a few chloroplasts suggesting that energy was used primarily for elongation. Thus, intercalary growth could be interpreted as a defense strategy during later stages of encrustation when photosynthetic activity diminishes due to surface coverage by Fe-precipitates and to provide the algae with new uncovered cell surfaces.

Production of EPS as a shunt mechanism should decline if less carbon is fixed during photosynthesis (Wotton, 2004) which provides a potential link between EPS production and *Gallionella* colonization. Brown algae contain fewer chloroplasts, indicating reduced photosynthetic activity and EPS production leading to a decrease in *Gallionella* cell number and Fe(II) oxidation on the algae surface. This study showed higher microbial diversity on the surface of brown *Tribonema* when lower numbers of *Gallionella* were detected. Some putative predators of algae, such as "*Candidatus* Odyssella" and *Cystobacteraceae* were also identified on the surface of the brown *Tribonema*. These predators colonize algae in order to consume material released upon cell lysis as a natural senescence process or under stress conditions (Levy et al., 2009). Algal EPS has been shown to function as a cell defense mechanism to protect cells from colonization of predators or pathogens (Steinberg et al., 1997), thus a reduced rate of EPS formation may lead to predator colonization.

BGD
12, 7705–7737, 2015

5 Summary and conclusion

The filamentous yellow-green algae (*Tribonema* sp.) were observed in the metal-contaminated groundwater outflow in the former Ronneburg uranium mining district, suggesting a tolerance to high metal concentrations and metal deposits. Cells of green algae were fully encrusted with Fe-oxides. The Fe-precipitates on the algae surfaces were predominantly colonized by *Gallionella*-related FeOB. *Gallionella*-related FeOB were abundant in the stream water and these bacteria appeared to be actively involved in Fe(II) oxidation. Thus, both sunlight and Fe(II) served as energy sources for primary producers in this slightly acidic stream promoting complex microbial interactions in the ochre deposits on the algal cells. EPS-like polymeric matrices, likely produced as a shunt for carbon during photosynthesis, provided a suitable microenvironment for the microaerophilic FeOB due to its high affinity for metal(loid)s and reduced oxygen diffusion. However, excess deposition of Fe-oxides appeared to be fatal for photosynthetic activities forcing intercalary elongation of the filaments. This defense response caused discontinuous deposition patterns of Fe-oxides as observed on the brown colored algae which showed lower number of chloroplasts. The reduced EPS production could have favored growth of algal predators on the brown algae and together with ochre deposition contributed to algal decline.

The Supplement related to this article is available online at doi:10.5194/bgd-12-7705-2015-supplement.

Author contributions. J. F. Mori and K. Küsel designed and J. F. Mori performed the experiments. T. R. Neu conducted CLSM imaging analysis. S. Lu carried out sampling and microscopic analysis with J. F. Mori. M. Händel and K. U. Totsche performed SEM-EDX and FTIR analysis. J. F. Mori prepared the manuscript with contributions from all co-authors.

Acknowledgements. The authors thank the graduate research training group “Alternation and element mobility at the microbe–mineral interface” (GRK 1257), which is part of the Jena School

BGD
12, 7705–7737, 2015

for Microbial Communication (JSMC) and funded by the Deutsche Forschungsgemeinschaft (DFG) for financial support. We would also like to thank Denise M. Akob and Georg Büchel for help during sampling. We appreciate Martina Herrmann for sequence analysis, Maren Sickinger for qPCR works, Dirk Merten for ICP measurements, Gundula Rudolph for DOC analysis, Steffen Kolb, Juanjuan Wang, and Maria Fabisch for helpful discussions and Rebecca Cooper for manuscript proofreading.

References

Akiyama, M., Ioriya, T., Imahori, K., Kasaki, H., Kumamoto, S., Kobayashi, H., Takahashi, E., Tsumura, K., Hirano, M., and Hirose, H.: Illustrations of the Japanese Fresh-Water Algae, Uchidarokakuho Publishing Company, Limited, 1977.

Azam, F.: Microbial control of oceanic carbon flux: the plot thickens, Science, 280, 694–695, 1998.

Bond, P. L., Smriga, S. P., and Banfield, J. F.: Phylogeny of microorganisms populating a thick, subaerial, predominantly lithotrophic biofilm at an extreme acid mine drainage site, Appl. Environ. Microb., 66, 3842–3849, doi:10.1128/aem.66.9.3842-3849.2000, 2000.

Bray, J. R. and Curtis, J. T.: An ordination of the upland forest communities of southern Wisconsin, Ecol. Monogr., 27, 325–349, 1957.

Cantonati, M. and Lowe, R. L.: Lake benthic algae: toward an understanding of their ecology, Freshwater, 33, 475–486, 2014.

Carlson, L., Bigham, J. M., Schwertmann, U., Kyek, A., and Wagner, F.: Scavenging of As from acid mine drainage by schwertmannite and ferrihydrite: a comparison with synthetic analogues, Environ. Sci. Technol., 36, 1712–1719, doi:10.1021/es0110271, 2002.

Chan, C. S., De Stasio, G., Welch, S. A., Girasole, M., Frazer, B. H., Nesterova, M. V., Fakra, S., and Banfield, J. F.: Microbial polysaccharides template assembly of nanocrystal fibers, Science, 303, 1656–1658, doi:10.1126/science.1092098, 2004.

Chapman, V. J.: An Introduction to the Study of Algae, Cambrige University Press, 387, 1941.

Cleare, M. and Percival, E.: Carbohydrates of the fresh water alga *Tribonema aequale*. I. Low molecular weight and polysaccharides, Brit. Phycol. J., 7, 185–193, doi:10.1080/00071617200650201, 1972.

Cole, J. J.: Interactions between bacteria and algae in aquatic ecosystems, Annu. Rev. Ecol. Syst., 13, 291–314, 1982.
Collier, K. and Winterbourn, M.: Structure of epilithon in some acidic and circumneutral streams in South Westland, New Zealand, New Zealand Natural Sciences, 17, 1–11, 1990.
Colmer, A. R. and Hinkle, M.: The role of microorganisms in acid mine drainage: a preliminary report, Science, 106, 253–256, 1947.
Courtin-Nomade, A., Grosbois, C., Bril, H., and Roussel, C.: Spatial variability of arsenic in some iron-rich deposits generated by acid mine drainage, Appl. Geochem., 20, 383–396, doi:10.1016/j.apgeochem.2004.08.002, 2005.
Das, B. K., Roy, A., Koschorreck, M., Mandal, S. M., Wendt-Potthoff, K., and Bhattacharya, J.: Occurrence and role of algae and fungi in acid mine drainage environment with special reference to metals and sulfate immobilization, Water Res., 43, 883–894, doi:10.1016/j.watres.2008.11.046, 2009.
Dorigo, U., Berard, A., and Humbert, J. F.: Comparison of eukaryotic phytobenthic community composition in a polluted river by partial 18S rRNA gene cloning and sequencing, Microb. Ecol., 44, 372–380, doi:10.1007/s00248-002-2024-x, 2002.
Emerson, D. and Moyer, C.: Isolation and characterization of novel iron-oxidizing bacteria that grow at circumneutral pH, Appl. Environ. Microb., 63, 4784–4792, 1997.
Emerson, D. and Weiss, J. V.: Bacterial iron oxidation in circumneutral freshwater habitats: findings from the field and the laboratory, Geomicrobiol. J., 21, 405–414, 2004.
Emerson, D., Weiss, J. V., and Megonigal, J. P.: Iron-oxidizing bacteria are associated with ferric hydroxide precipitates (Fe-plaque) on the roots of wetland plants, Appl. Environ. Microb., 65, 2758–2761, 1999.
Emerson, D., Field, E., Chertkov, O., Davenport, K., Goodwin, L., Munk, C., Nolan, M., and Woyke, T.: Comparative genomics of freshwater Fe-oxidizing bacteria: implications for physiology, ecology, and systematics, Front. Microbiol., 4, 254, doi:10.3389/fmicb.2013.00254, 2013.
Euringer, K., and Lueders, T.: An optimised PCR/T-RFLP fingerprinting approach for the investigation of protistan communities in groundwater environments, J. Microbiol. Meth., 75, 262–268, doi:10.1016/j.mimet.2008.06.012, 2008.
Fabisch, M., Beulig, F., Akob, D. M., and Küsel, K.: Surprising abundance of *Gallionella*-related iron oxidizers in creek sediments at pH 4.4 or at high heavy metal concentrations, Front. Microbiol., 4, 390, doi:10.3389/fmicb.2013.00390, 2013.

BGD
12, 7705–7737, 2015

Fabisch, M., Freyer, G., Johnson, C. A., Büchel, G., Akob, D. M., Neu, T. R., and Küsel, K.: Dominance of "*Gallionella capsiferriformans*" and heavy metal association with *Gallionella*-like stalks in metal-rich pH 6 mine water discharge, Geobiology, submitted, 2015.

Fisher, M., Zamir, A., and Pick, U.: Iron uptake by the halotolerant alga *Dunaliella* is mediated by a plasma membrane transferrin, J. Biol. Chem., 273, 17553–17558, 1998.

Foster, P. L.: Copper exclusion as a mechanism of heavy metal tolerance in a green alga, Nature, 269, 322–323, 1977.

Foster, P. L.: Metal resistances of *Chlorophyta* from rivers polluted by heavy metals, Freshwater Biol., 12, 41–61, 1982.

Gebühr, C., Pohlon, E., Schmidt, A., and Küsel, K.: Development of microalgae communities in the phytotelmata of allochthonous populations of *Sarracenia purpurea* (Sarraceniaceae), Plant Biol., 8, 849–860, 2006.

Geesey, G., Mutch, R., Costerton, J. T., and Green, R.: Sessile bacteria: an important component of the microbial population in small mountain streams, Limnol. Oceanogr., 23, 1214–1223, 1978.

Greene, B., McPherson, R., and Darnall, D.: Algal sorbents for selective metal ion recovery, in: Metals Speciation, Separation, and Recovery, Lewis Publishers, Chelsea, MI, 315–338, 1987.

Gudleifsson, B. E.: *Tribonema viride* (*Xanthophyta*) on cultivated grassland during winter and spring, Acta Botanica Islandica, 7, 27–30, 1984.

Haack, T. K. and McFeters, G. A.: Microbial dynamics of an epilithic mat community in a high alpine stream, Appl. Environ. Microb., 43, 702–707, 1982.

Hallberg, K. B., Coupland, K., Kimura, S., and Johnson, D. B.: Macroscopic streamer growths in acidic, metal-rich mine waters in north wales consist of novel and remarkably simple bacterial communities, Appl. Environ. Microb., 72, 2022–2030, doi:10.1128/aem.72.3.2022-2030.2006, 2006.

Hanert, H. H.: The genus *Gallionella*, in: The Prokaryotes, Springer Verlag, New York, 990–995, 2006.

Hedrich, S., Lunsdorf, H., Keeberg, R., Heide, G., Seifert, J., and Schlomann, M.: Schwertmannite formation adjacent to bacterial cells in a mine water treatment plant and in pure cultures of *Ferrovum myxofaciens*, Environ. Sci. Technol., 45, 7685–7692, doi:10.1021/es201564g, 2011a.

BGD
12, 7705–7737, 2015

Hedrich, S., Schlomann, M., and Johnson, D. B.: The iron-oxidizing proteobacteria, Microbiology, 157, 1551–1564, doi:10.1099/mic.0.045344-0, 2011b.
Heinzel, E., Janneck, E., Glombitza, F., Schlömann, M., and Seifert, J.: Population dynamics of iron-oxidizing communities in pilot plants for the treatment of acid mine waters, Environ. Sci. Technol., 43, 6138–6144, 2009.
Jiao, Y., Cody, G. D., Harding, A. K., Wilmes, P., Schrenk, M., Wheeler, K. E., Banfield, J. F., and Thelen, M. P.: Characterization of extracellular polymeric substances from acidophilic microbial biofilms, Appl. Environ. Microb., 76, 2916–2922, doi:10.1128/aem.02289-09, 2010.
Johnson, C. A., Freyer, G., Fabisch, M., Caraballo, M. A., Küsel, K., and Hochella, M. F.: Observations and assessment of iron oxide and green rust nanoparticles in metal-polluted mine drainage within a steep redox gradient, Environ. Chem., 11, 377–391, doi:10.1071/EN13184, 2014.
Johnson, D. B. and Hallberg, K. B.: Carbon, iron and sulfur metabolism in acidophilic microorganisms, Adv. Microb. Physiol., 54, 201–255, doi:10.1016/s0065-2911(08)00003-9, 2009.
Johnson, D. B., Hallberg, K. B., and Hedrich, S.: Uncovering a microbial enigma: isolation and characterization of the streamer-generating, iron-oxidizing, acidophilic bacterium "*Ferrovum myxofaciens*", Appl. Environ. Microb., 80, 672–680, 2014.
Johnsongreen, P. C. and Crowder, A. A.: Iron-oxide deposition on axenic and non-axenic roots of rice seedlings (*Oryza sativa* L.), J. Plant Nutr., 14, 375–386, doi:10.1080/01904169109364209, 1991.
Kappler, A. and Straub, K. L.: Geomicrobiological cycling of iron, Rev. Mineral. Geochem., 59, 85–108, 2005.
Kay, C. M., Rowe, O., Rocchetti, L., Coupland, K., Hallberg, K., and Johnson, D.: Evolution of microbial "streamer" growths in an acidic, metal-contaminated stream draining an abandoned underground copper mine, Life (Basel), 3, 189–210, 2013.
Kozubal, M. A., Macur, R. E., Jay, Z. J., Beam, J. P., Malfatti, S. A., Tringe, S. G., Kocar, B. D., Borch, T., and Inskeep, W. P.: Microbial iron cycling in acidic geothermal springs of Yellowstone National Park: integrating molecular surveys, geochemical processes, and isolation of novel Fe-active microorganisms, Front. Microbiol., 3, 109, doi:10.3389/fmicb.2012.00109, 2012.
Leduc, L. G. and Ferroni, G. D.: The chemolithotrophic bacterium *Thibacillus ferrooxidans*, FEMS Microbiol. Rev., 14, 103–119, 1994.

BGD
12, 7705–7737, 2015

Levy, J., Stauber, J. L., Wakelin, S. A., and Jolley, D. F.: The effect of bacteria on the sensitivity of microalgae to copper in laboratory bioassays, Chemosphere, 74, 1266–1274, doi:10.1016/j.chemosphere.2008.10.049, 2009.
Liu, H. and Buskey, E. J.: Hypersalinity enhances the production of extracellular polymeric substance (EPS) in the Texas brown tide alga, *Aureoumbra lagunensis* (Pelagophyceae), J. Phycol., 36, 71–77, 2000.
López-Archilla, A. I., Marin, I., and Amils, R.: Microbial community composition and ecology of an acidic aquatic environment: the Tinto River, Spain, Microb. Ecol., 41, 20–35, 2001.
Lüdecke, C., Reiche, M., Eusterhues, K., Nietzsche, S., and Küsel, K.: Acid-tolerant microaerophilic Fe(II)-oxidizing bacteria promote Fe(III)-accumulation in a fen, Environ. Microbiol., 12, 2814–2825, doi:10.1111/j.1462-2920.2010.02251.x, 2010.
Machova, K., Elster, J., and Adamec, L.: Xanthophyceaen assemblages during winter-spring flood: autecology and ecophysiology of *Tribonema fonticolum* and *T. monochloron*, Hydrobiologia, 600, 155–168, doi:10.1007/s10750-007-9228-5, 2008.
Malik, A.: Metal bioremediation through growing cells, Environ. Int., 30, 261–278, 2004.
Neu, T. R., Swerhone, G. D., and Lawrence, J. R.: Assessment of lectin-binding analysis for in situ detection of glycoconjugates in biofilm systems, Microbiology, 147, 299–313, 2001.
Neubauer, S. C., Emerson, D., and Megonigal, J. P.: Life at the energetic edge: kinetics of circumneutral iron oxidation by lithotrophic iron-oxidizing bacteria isolated from the wetland-plant rhizosphere, Appl. Environ. Microb., 68, 3988–3995, doi:10.1128/aem.68.8.3988-3995.2002, 2002.
Peine, A., Tritschler, A., Küsel, K., and Peiffer, S.: Electron flow in an iron-rich acidic sediment - evidence for an acidity-driven iron cycle, Limnol. Oceanogr., 45, 1077–1087, 2000.
Reed, R. and Gadd, G.: Metal tolerance in eukaryotic and prokaryotic algae, in: Heavy Metal Tolerance in Plants: Evolutionary Aspects, 105–118, CRC press, Boca Raton, FL, 1989.
Roth, R. I., Panter, S. S., Zegna, A. I., and Levin, J.: Bacterial endotoxin (lipopolysaccharide) stimulates the rate of iron oxidation, J. Endotoxin Res., 6, 313–319, 2000.
Rowe, O. F., Sanchez-Espana, J., Hallberg, K. B., and Johnson, D. B.: Microbial communities and geochemical dynamics in an extremely acidic, metal-rich stream at an abandoned sulfide mine (Huelva, Spain) underpinned by two functional primary production systems, Environ. Microbiol., 9, 1761–1771, doi:10.1111/j.1462-2920.2007.01294.x, 2007.
Schloss, P. D., Westcott, S. L., Ryabin, T., Hall, J. R., Hartmann, M., Hollister, E. B., Lesniewski, R. A., Oakley, B. B., Parks, D. H., and Robinson, C. J.: Introducing mothur: open-

BGD
12, 7705–7737, 2015

source, platform-independent, community-supported software for describing and comparing microbial communities, Appl. Environ. Microb., 75, 7537–7541, 2009.
Sengbusch, P. V. and Müller, U.: Distribution of glycoconjugates at algal cell surfaces as monitored by FITC-conjugated lectins. Studies on selected species from *Cyanophyta*, *Pyrrhophyta*, *Raphidophyta*, *Euglenophyta*, *Chromophyta*, and *Chlorophyta*, Protoplasma, 114, 103–113, 1983.
Senko, J. M., Wanjugi, P., Lucas, M., Bruns, M. A., and Burgos, W. D.: Characterization of Fe (II) oxidizing bacterial activities and communities at two acidic Appalachian coalmine drainage-impacted sites, ISME J., 2, 1134–1145, 2008.
Smith, G. M.: Cryptogamic Botany, Vol. 1, Algae and Fungi, McGraw-Hill, New York, 1938.
Steinberg, P. D., Schneider, R., and Kjelleberg, S.: Chemical defenses of seaweeds against microbial colonization, Biodegradation, 8, 211–220, doi:10.1023/a:1008236901790, 1997.
Stevenson, R. J., Bothwell, M. L., Lowe, R. L., and Thorp, J. H.: Algal Ecology: Freshwater Benthic Ecosystem, Academic press, San Diego, 1996.
Tabatabai, M. A.: A rapid method for determination of sulfate in water samples, Environ. Lett., 7, 237–243, 1974.
Tamura, H., Goto, K., Yotsuyan, T., and Nagayama, M.: Spectrophotometric determination of iron(II) with 1,10-phenanthroline in presence of large amounts of iron(III), Talanta, 21, 314–318, doi:10.1016/0039-9140(74)80012-3, 1974.
Tang, Y. Z. and Dobbs, F. C.: Green autofluorescence in dinoflagellates, diatoms, and other microalgae and its implications for vital staining and morphological studies, Appl. Environ. Microb., 73, 2306–2313, doi:10.1128/aem.01741-06, 2007.
Transeau, E. N.: The periodicity of freshwater algae, Am. J. Bot., 3, 121–133, 1916.
Tyson, G. W., Chapman, J., Hugenholtz, P., Allen, E. E., Ram, R. J., Richardson, P. M., Solovyev, V. V., Rubin, E. M., Rokhsar, D. S., and Banfield, J. F.: Community structure and metabolism through reconstruction of microbial genomes from the environment, Nature, 428, 37–43, doi:10.1038/nature02340, 2004.
Vinocur, A. and Izaguirre, I.: Freshwater algae (excluding *Cyanophyceae*) from nine lakes and pools of Hope Bay, Antarctic Peninsula, Antarct. Sci., 6, 483–490, 1994.
Wakao, N., Tachibana, H., Tanaka, Y., Sakurai, Y., and Shiota, H.: Morphological and physiological-characterstics of streamers in acid-mine drainage water from a pyritic mine, J. Gen. Appl. Microbiol., 31, 17–28, doi:10.2323/jgam.31.17, 1985.

BGD
12, 7705–7737, 2015

Wang, H., Ji, B., Wang, J., Guo, F., Zhou, W., Gao, L., and Liu, T.: Growth and biochemical composition of filamentous microalgae *Tribonema* sp. as potential biofuel feedstock, Bioproc. Biosyst. Eng., 37, 2607–2613, 2014.

Warner, R. W.: Distribution of biota in a stream polluted by acid mine-drainage, Ohio J. Sci.,71, 202–215, 1971.

Wiegert, R. G. and Mitchell, R.: Ecology of Yellowstone thermal effluent systems: intersects of blue-green algae, grazing flies (*Paracoenia*, Ephydridae) and water mites (*Partnuniella*, Hydrachnellae), Hydrobiologia, 41, 251–271, 1973.

Winterbourn, M. J., McDiffett, W. F., and Eppley, S. J.: Aluminium and iron burdens of aquatic biota in New Zealand streams contaminated by acid mine drainage: effects of trophic level, Sci. Total Environ., 254, 45–54, doi:10.1016/s0048-9697(00)00437-x, 2000.

Wotton, R. S.: The utiquity and many roles of exopolymers (EPS) in aquatic systems, Sci. Mar., 68, 13–21, 2004.

Yu, Q., Matheickal, J. T., Yin, P., and Kaewsarn, P.: Heavy metal uptake capacities of common marine macro algal biomass, Water Res., 33, 1534–1537, 1999.

BGD
12, 7705–7737, 2015

Table 1. Average 16S rRNA gene copy numbers of *Gallionella* detected per gram wet weight algae sampled at sites O, A, B, and C, and at three sampling times in 2013 and measured by quantitative PCR (n = 3, ±SD).

	Site O	Site A	Site B	Site C
Jul 2013	Not reachable	Green $1.85 \times 10^9 \pm 1.86 \times 10^7$	Green $1.72 \times 10^9 \pm 1.62 \times 10^8$	Brown $0.95 \times 10^9 \pm 6.66 \times 10^7$
Aug 2013	Green $6.78 \times 10^9 \pm 2.36 \times 10^8$	Green $7.08 \times 10^9 \pm 3.76 \times 10^8$	Brown $1.45 \times 10^9 \pm 1.07 \times 10^8$	Brown $1.25 \times 10^9 \pm 1.62 \times 10^7$
Sep 2013	Green $2.25 \times 10^9 \pm 1.19 \times 10^7$	Brown $1.10 \times 10^9 \pm 3.47 \times 10^7$	No algae	No algae

BGD
12, 7705–7737, 2015

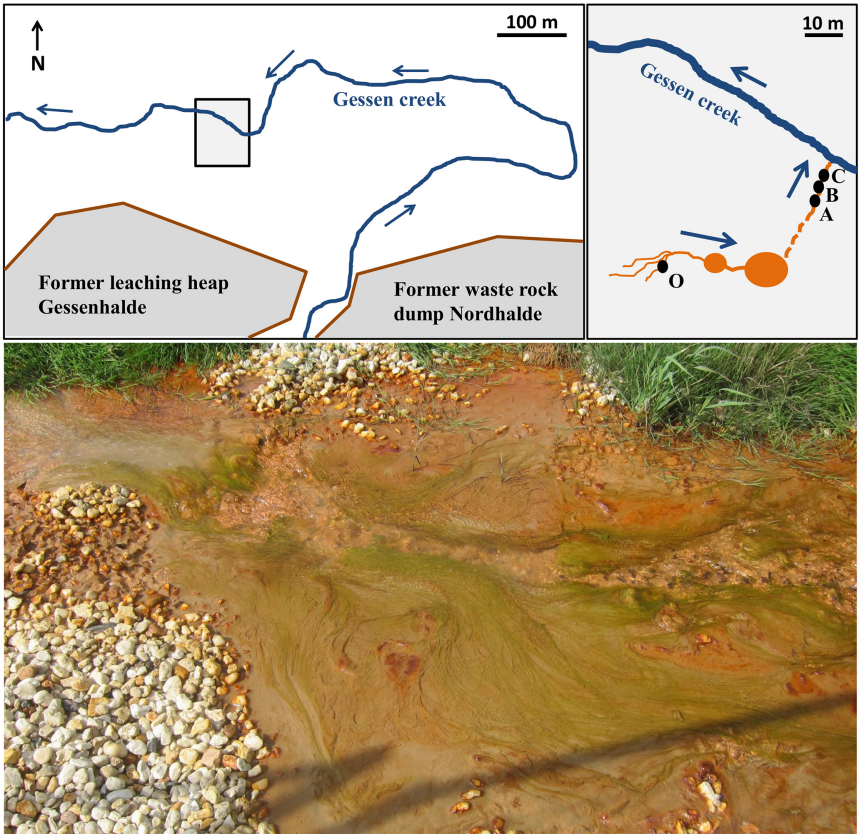

Figure 1. Schematic maps of the study site and photograph of the site A in the former Ronneburg uranium mining district (Thuringia, Germany). Maps show the locations of sampling sites O, A, B and C on the grassland close to Gessen creek. Blue arrows indicate the flow direction of the creek and outflow streams. The photograph was taken in September 2011 and shows the presence of conspicuous green filamentous algae.

BGD
12, 7705–7737, 2015

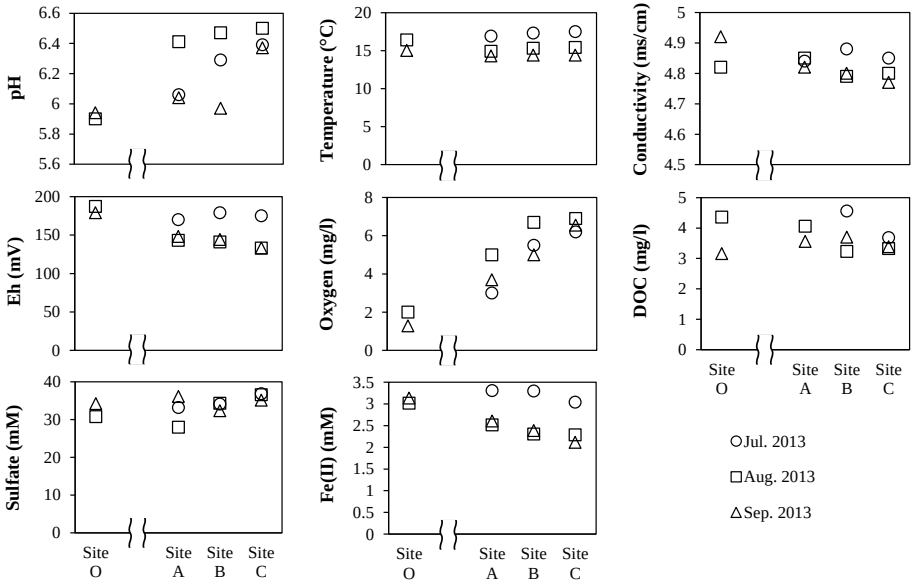

Figure 2. Chemical parameters of water at each sampling site in the outflow water stream. Water pH, oxygen, temperature, conductivity and Eh were measured in the field at site O, A, B and C in July, August, and September 2013. Concentrations of organic carbon, sulfate and Fe(II) were determined later in the laboratory.

BGD
12, 7705–7737, 2015

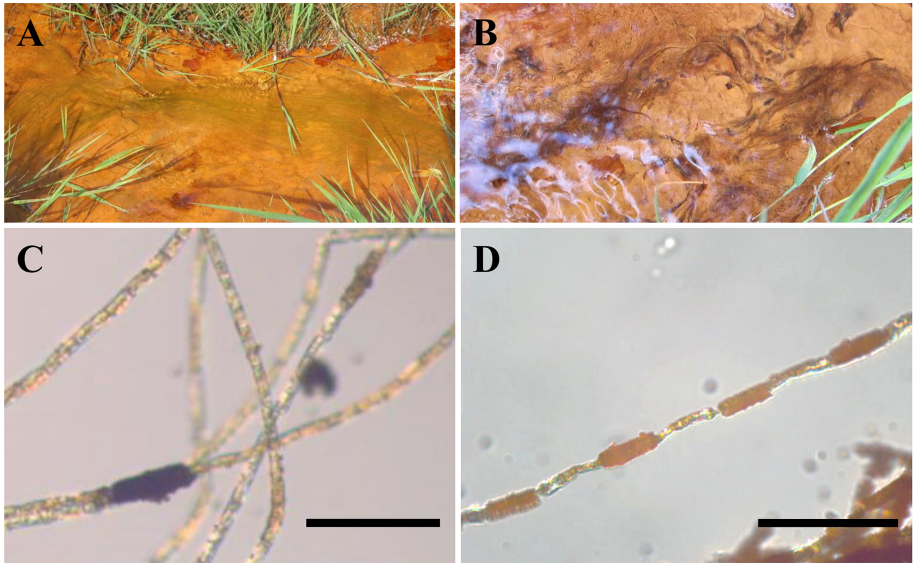

Figure 3. Photographs **(a, b)** and light microscopic pictures **(c, d)** of the green algae in site A **(a, c)** and the brown algae in site C **(b, d)** taken in July 2013. The microscopic pictures show Fe-mineral precipitates on the algae. Scale bars indicate 100 µm.

BGD
12, 7705–7737, 2015

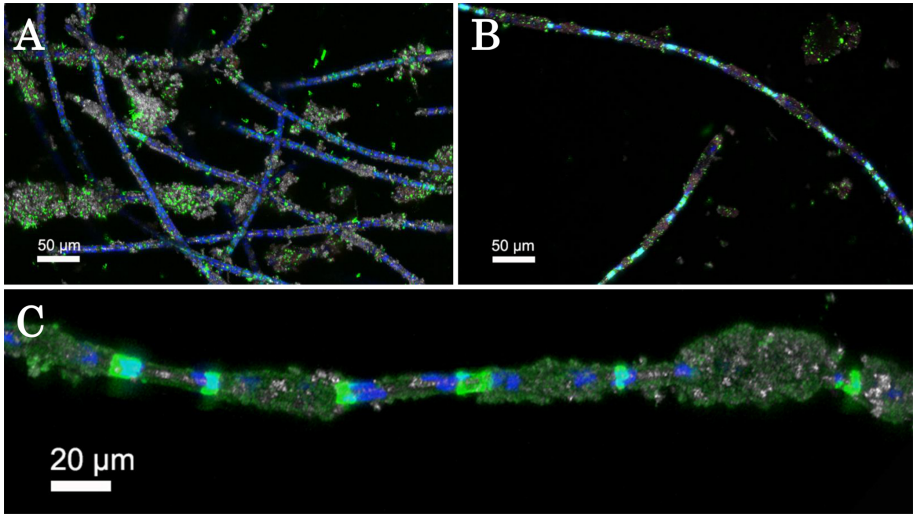

Figure 4. Confocal laser scanning microscopy images of the algae-microbial communities collected at site O (outflow) of the stream in September 2013. Maximum intensity projection of the green algae **(a)** and the brown algae **(b)** stained with Syto9 were recorded (color allocation: green – nucleic acid stain; blue – autofluorescence of chlorophyll *a*; grey – reflection). Brown algae stained with AAL-Alexa448 **(c)** shows glycoconjugates (green), autofluorescence of chlorophyll *a* (blue), and refection (grey).

BGD
12, 7705–7737, 2015

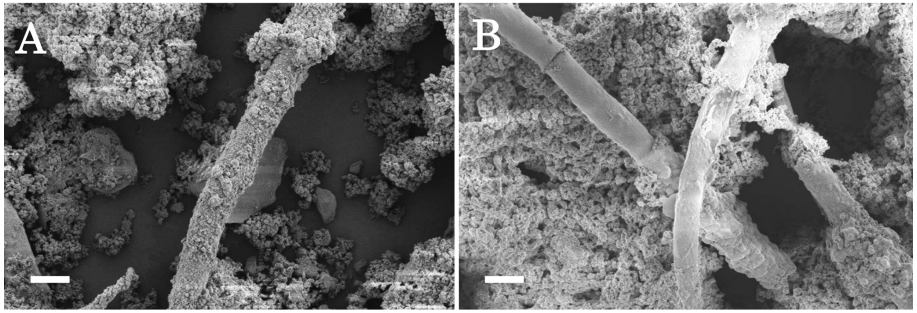

Figure 5. Scanning electron microscopy images of the green algae in site O **(a)** and the brown algae in site A **(b)** taken in September 2013. Scale bars indicate 10 µm.

BGD
12, 7705–7737, 2015

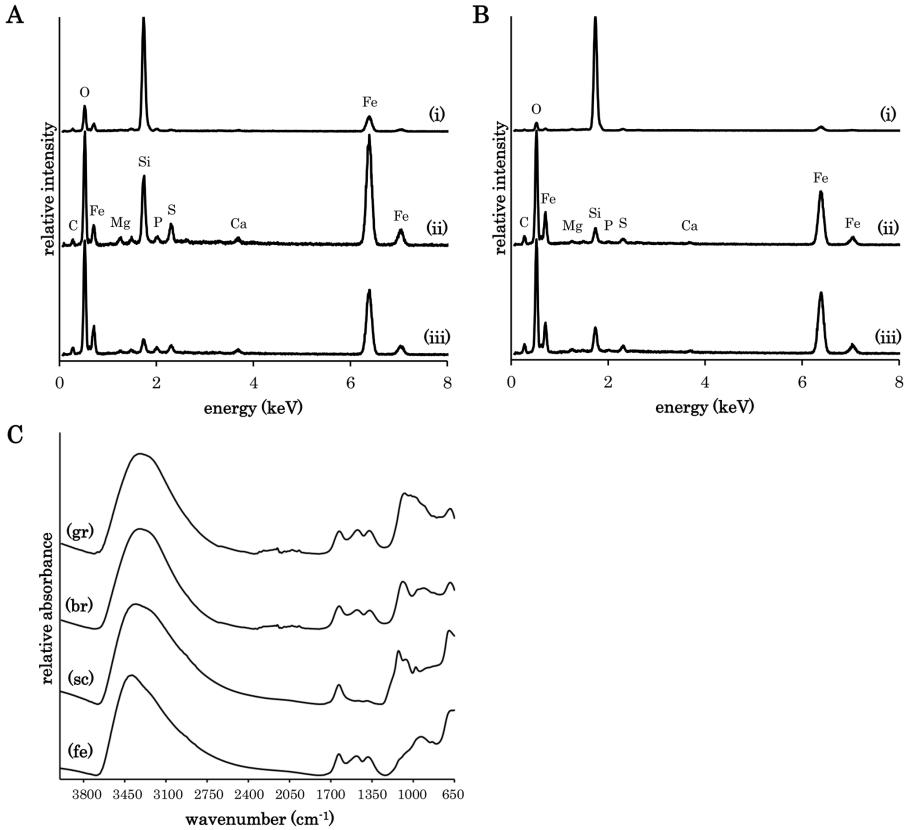

Figure 6. EDX and FTIR spectra of minerals precipitated around the algae. EDX spectra of minerals around the green algae **(a)** and the brown algae **(b)** were recorded on the non-encrusted algal surface (i), the encrusted algal surface (ii) and Fe-oxides which were not connected to the algae (iii). FTIR spectra of Fe-oxides **(c)** were recorded on the green algae (gr) and the brown algae (br), comparing with spectra of schwertmannite (sc) and ferrihydrite (fe) as references.

BGD
12, 7705–7737, 2015

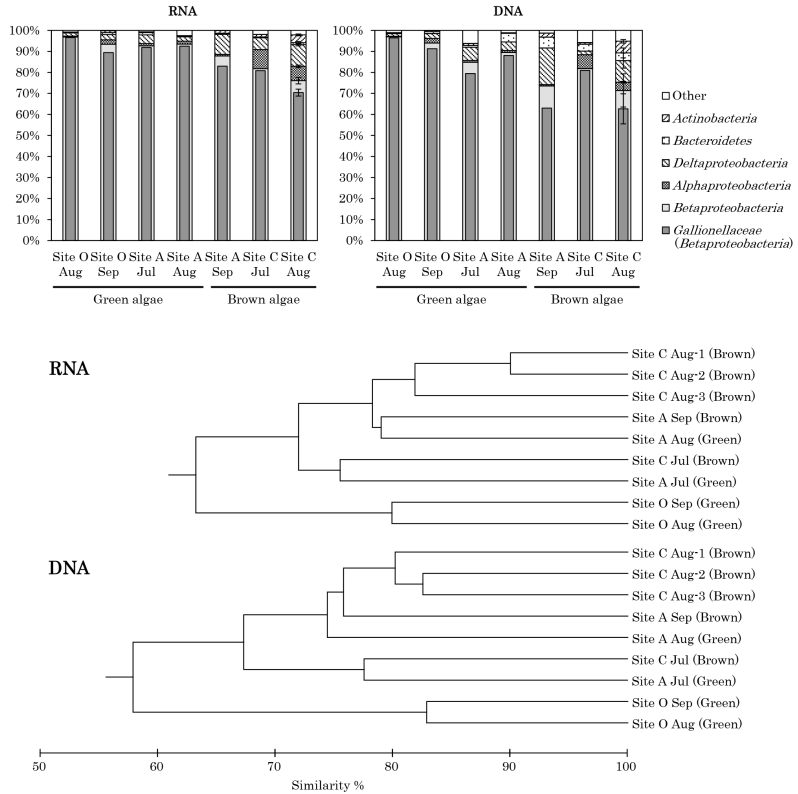

Figure 7. Bacterial community compositions obtained from algal samples detected by 16S rRNA gene-targeted amplicon pyrosequencing (above) and dendrograms indicating similarities of RNA and DNA compositions (below). Calculations of the bacterial populations were based on the total numbers of OTUs associated with phylotypes of sequenced representatives at the phylum level, or class level for Proteobacteria. Percentages of *Gallionellaceae* (*Betaproteobacteria*) were also shown. (n = 1; Site C August, n = 3, error bars indicate SD).

BGD
12, 7705–7737, 2015